Downloaded from orbit.dtu.dk on: Apr 24, 2024

DTU Library

Cs-131 as an experimental tool for the investigation and quantification of the radiotoxicity of intracellular Auger decays in vitro

Fredericia, Pil M.; Siragusa, Mattia; Köster, Ulli; Severin, Gregory; Groesser, Torsten; Jensen, Mikael

Published in:
International Journal of Radiation Biology

Link to article, DOI:
10.1080/09553002.2020.1787541

Publication date:
2023

Document Version
Publisher's PDF, also known as Version of record

Link back to DTU Orbit

Citation (APA):
Fredericia, P. M., Siragusa, M., Köster, U., Severin, G., Groesser, T., & Jensen, M. (2023). Cs-131 as an experimental tool for the investigation and quantification of the radiotoxicity of intracellular Auger decays in vitro. *International Journal of Radiation Biology*, *99*(1). https://doi.org/10.1080/09553002.2020.1787541

General rights
Copyright and moral rights for the publications made accessible in the public portal are retained by the authors and/or other copyright owners and it is a condition of accessing publications that users recognise and abide by the legal requirements associated with these rights.

- Users may download and print one copy of any publication from the public portal for the purpose of private study or research.
- You may not further distribute the material or use it for any profit-making activity or commercial gain
- You may freely distribute the URL identifying the publication in the public portal

If you believe that this document breaches copyright please contact us providing details, and we will remove access to the work immediately and investigate your claim.

International Journal of Radiation Biology

ISSN: (Print) (Online) Journal homepage: https://www.tandfonline.com/loi/irab20

Cs-131 as an experimental tool for the investigation and quantification of the radiotoxicity of intracellular Auger decays in vitro

Pil M. Fredericia, Mattia Siragusa, Ulli Köster, Gregory Severin, Torsten Groesser & Mikael Jensen

To cite this article: Pil M. Fredericia, Mattia Siragusa, Ulli Köster, Gregory Severin, Torsten Groesser & Mikael Jensen (2023) Cs-131 as an experimental tool for the investigation and quantification of the radiotoxicity of intracellular Auger decays in vitro, International Journal of Radiation Biology, 99:1, 39-52, DOI: 10.1080/09553002.2020.1787541

To link to this article: https://doi.org/10.1080/09553002.2020.1787541

Copyright © 2020 The Author(s). Published with license by Taylor & Francis Group, LLC.

Published online: 15 Jul 2020.

Submit your article to this journal

Article views: 808

View related articles

View Crossmark data

Citing articles: 2 View citing articles

Full Terms & Conditions of access and use can be found at
https://www.tandfonline.com/action/journalInformation?journalCode=irab20

INTERNATIONAL JOURNAL OF RADIATION BIOLOGY
2023, VOL. 99, NO. 1, 39–52
https://doi.org/10.1080/09553002.2020.1787541

Taylor & Francis
Taylor & Francis Group

ORIGINAL ARTICLE

OPEN ACCESS Check for updates

Cs-131 as an experimental tool for the investigation and quantification of the radiotoxicity of intracellular Auger decays in vitro

Pil M. Fredericia[a], Mattia Siragusa[a], Ulli Köster[b], Gregory Severin[a], Torsten Groesser[a], and Mikael Jensen[a]

[a]The Hevesy Laboratory, DTU-Nutech, Roskilde, Denmark; [b]Department of Chemistry, Institut Laue-Langevin, Grenoble, France

ABSTRACT

Purpose: In this work, we set out to provide an experimental setup, using Cs-131, with associated dosimetry for studying relative biological effectiveness (RBE) of Auger emitters.

Material and methods: Cs-131 decays by 100% electron capture producing K- (9%) and L- (80%) Auger electrons with mean energies of 26 keV and 3.5 keV, respectively, plus ≈ 9.4 very low energy electrons (<0.5 keV) per decay. Cs-131 accumulates in the cells through the Na^+/K^+-ATPase. By this uptake mechanism and the alkali chemistry of Cs^+, we argue for its intracellular homogeneous distribution. Cs-131 was added to the cell culture medium of HeLa and V79 Cells. The bio-kinetics of Cs-131 (uptake, release, intracellular distribution) was examined by measuring its intracellular activity concentration over time. Taking advantage of the 100% confluent cellular monolayer, we developed a new and robust dosimetry that is entrusted to a quantity called S_C-value.

Results: The S_C-values evaluated in the cell nucleus are almost independent of the nuclear size and geometry. We obtained dose-rate controlled RBE-values for intracellular Cs-131 decay. Using the γH2AX assay, the RBE was 1 for HeLa cells. Using the clonogenic cell survival, it was 3.9 for HeLa cells and 3.2 for V79 cells.

Conclusion: This experimental setup and dosimetry provides reliable RBE-values for Auger emitters in various cell lines.

ARTICLE HISTORY
Received 15 July 2019
Revised 22 May 2020
Accepted 3 June 2020

KEYWORDS
Auger emitters; RBE; Cs-131; S_C-value; cellular S-value

Introduction

The radiotoxic effects of Auger electrons have been investigated since the late 1960s-early 70 s when the first cell studies with I-125 were performed (Feinendegen et al. 1971; Hofer and Hughes 1971). The increased radiotoxicity of Auger-electron emitters is a result of the simultaneous emission of several low-energy electrons during a single decay. Because of the low energy and the related short contorted path, these electrons deposit their energy within nm to μm range from the decay site of the radionuclide. This results in a high local energy deposition density, comparable to that produced by high LET radiation. If the decay happens in close proximity to the DNA, severe DNA damage is induced (Kassis and Adelstein 2005). Consequently, Auger-electron emitting radionuclides have the potential to damage single targeted cells while sparing the neighboring ones. This has led to the idea of using Auger-electron emitting radionuclides in targeted radionuclide therapy against cancer (Kassis 2004).

Great progress has been made in recent years in delivering Auger emitters specifically to the cell nucleus, utilizing receptor-mediated uptake and nuclear localization signal (Costantini et al. 2007; Leyton et al. 2011; Hoang et al. 2012). Nuclear localization is believed to be a requirement for successful Auger radionuclide therapy and the delivery and radiotoxicity of I-125, In-111 and Tc-99m have been studied intensely (Kassis 2003). Unfortunately, these radionuclides are, due to their chemistry, all prone to a complicated intracellular fate. Chemical modifications and delabelling of the ligand and/or incorporation of the radionuclide into metabolites can result in a complex intracellular distribution. Consequently, the already complex absorbed dose calculations becomes even more problematic and subject to high uncertainties. Without a correct calculation of the absorbed dose at the cellular level, the radiotoxicity of Auger emitters cannot be properly quantified. In light of this, we here propose the use of a 'new' radionuclide, Cs-131, for in vitro experiments investigating the radiotoxicity of Auger emitters. Even though Cs-131 is not suitable for systemic radionuclide therapy in clinical or preclinical settings (because of its alkali chemistry), it has several characteristics that makes it a highly suitable 'model' isotope for in vitro studies of Auger-electron radiobiology.

CONTACT Pil M. Fredericia pilf@dtu.dk The Hevesy Laboratory, Center for Nuclear Technologies, Technical University of Denmark, Building 202, Frederiksborgvej 399, Roskilde, 4000, Denmark

Copyright © 2020 The Author(s). Published with license by Taylor & Francis Group, LLC.
This is an Open Access article distributed under the terms of the Creative Commons Attribution-NonCommercial License (http://creativecommons.org/licenses/by-nc/4.0/), which permits unrestricted non-commercial use, distribution, and reproduction in any medium, provided the original work is properly cited.

Cs-131 is a 'pure' Auger-electron emitter, in the sense that it does not emit any significant β-radiation or conversion electrons. It has a half-life of 9.689 days and decays by electron capture (100%). In that process, an Auger K-electron with a mean energy of 26 keV (9%) and/or an Auger L-electron with a mean energy of 3.5 keV (80%) are emitted (NuDat2.72.7 2004). In the subsequent cascade, Auger-electrons of higher shells can also be emitted together with several Coster-Kronig and super Coster-Kronig electrons (often referred to as Auger-electrons). Overall an average of 10 electrons is released per decay, with an average energy of 0.6 keV per electron. Cs-131 decays to stable Xe-131 avoiding the complexity of further decay chain activity (NuDat2.72.7 2004).

As shown in this article, Cs-131 can readily be formed from reactor-produced Ba-131, using a simple 'solution generator' principle. This allows repeated biological experiments using the same irradiated batch of barium. Importantly, its alkali chemistry and the similarity to potassium in biological settings makes Cs-131 unlikely to be incorporated into biological molecules (Ussing 1959; Whittam and Ager 1964; Williams 1970; Davis et al. 1988; Avery 1995). Therefore, it should remain as a fully dissociated Cs^+ ion inside the cell.

In this article, we demonstrate the use of Cs-131 for in vitro radiobiology research. We investigate its bio-kinetics and based on the obtained results and on its known alkali chemistry, argue for a homogeneous intracellular distribution. In order to obtain robust absorbed dose calculations for Cs-131 in realistic cellular geometries, we define the so-called S_C-values (where C means 'concentration dependent'). With respect to cellular S-values, S_C-values are defined to be much less sensitive to variations in cellular dimensions. Therefore, they are less affected by the great biological variability of cellular and nuclear shapes and sizes.

We have demonstrated a new the experimental setup to obtain dose-rate controlled relative biological effectiveness (RBE)-values for intracellular Cs-131 decays in HeLa and V79 cells using γH2AX assay and clonogenic cell survival.

Material and methods

Production of Cs-131

Ba-131 (11.5 days half-life) was produced by high flux neutron bombardment at the ILL reactor (Institute Laue-Langevin, Grenoble, France) during 6–10 days at thermal neutron fluxes $(1.1–1.3)\cdot10^{15}\,cm^{-2}\,s^{-1}$ of either natural barium (25 mg carbonate, i.e. 17.4 mg barium) or 49% enriched Ba-130 (0.15 mg as nitrate). The irradiated targets were dissolved in hydrochloric acid, neutralized and re-precipitated with ammonium carbonate. The supernatant was spiked with sodium hydroxide, then dried and fired, leaving Cs-131 as a chloride salt with NaCl carrier. The re-precipitated targets were stored for 1–2 weeks for buildup of Cs-131, and then, the process could be repeated. We have milked up to 4 batches of useful Cs-131 activity from a single activated barium batch from ILL. The harvested Cs-131/NaCl salt was dissolved in hepes (Sigma-Aldrich, Brøndby, Denmark; for the bio-kinetic studies), or in PBS (Sigma-Aldrich) or water (for radiotoxicity assays) and pH was adjusted to ~7.

Liquid scintillation counting

Cs-131 activity was measured by liquid scintillation counting (LSC) using the Hidex 300SL (Hidex, Turku, Finland). Samples (of maximum 1 ml volume) were added to oximate glass vials (PerkinElmer, Skovlunde, Denmark) containing 10 ml ultima gold scintillation fluid (PerkinElmer) and shaken thoroughly to ensure a proper mixing. Samples were counted using channel 218–480 covering approximate 7–60 keV, (K-Auger branch and possible K-X-ray interactions in the scintillation cocktail). The spectrometer was operated in the triple-double coincidence mode to minimize background and lower any quenching effects. The background was measured using a blank. To convert CPS to Bq a standard sample of Cs-131 was measured on a germanium X-ray detector (GMX 35195, Ortec, US). This was efficiency calibrated against a calibrated and traceable Am-241 source (40.7 kBq at the time of the efficiency calibration; AEA Technology QSA GmbH, Braunschweig, Germany) using the 26.3 keV and 59.5 keV X-rays from Am-241 and the 29.5 keV and 29.8 keV X-rays from Cs-131.

Cell culture

HeLa cells (human cervical cancer cell line, ECACC 93021013) were obtained from ECACC, Salisbury, UK through Sigma-Aldrich (St Louis, MO). V79 cells (Chinese hamster lung fibroblasts) were a generous gift from Dr. Priscilla K. Cooper (LBNL, Berkeley, CA, USA). Both cell lines were cultivated in DMEM medium (Sigma-Aldrich, Brøndby, Denmark) supplemented with 10% FBS (Sigma-Aldrich), 4 mM L-Glutamine (Sigma-Aldrich) and 1% (v/v) antibiotic/antimycotic solution (working concentration: 100 U/ml penicillin, 0.1 mg/ml streptomycin, 0.25 μg/ml amphotericin B; Sigma-Aldrich) in a humidified atmosphere containing 5% CO_2 at 37 °C (ESCO Cell Culture CO2 incubator, Holm & Halby, Brøndby, Denmark).

Cellular kinetics of Cs-131

For all experiments, Cs-131 was added to the cell culture in the form of CsCl (dissolved) and mixed with growth medium (DMEM, 10% FBS, 4 mM L-glutamine and 1% antibiotic, antimycotic). Cs-131 activity was measured by LSC and the data decay corrected to the beginning of measurement. The number of cells and their size/volume was measured using the Sceptor 2.0 Cell Counter from Millipore (Merck Millipore Darmstadt, Germany), unless otherwise stated.

Uptake of Cs-131 by the cells

HeLa and V79 cells were seeded in 48-well plates (Sarstedt, Nümbrecht, Germany) and grown overnight. The cells were washed with PBS (Sigma-Aldrich) and incubated with Cs-

131 at activity concentrations of 20 kBq/ml to 17 MBq/ml, for up to 8 h (in one case 24 h) at 37 °C, 5% CO_2. After incubation, the cells were washed with PBS and trypsinized, using 0.1% trypsin (Gibco/ThermoFisher, Waltham, MA, USA) added 0.5 mM EDTA (Sigma-Aldrich) in PBS, for 3–5 min at 37 °C, 5% CO_2. The cells were re-suspended in growth medium and the number of cells, their sizes and the Cs-131 activity measured for each sample. A control for the washing efficiency was made in which Cs-131 was added and immediately removed from the cells. The Cs-131 activity in this control was subtracted from the other samples. Dividing the Cs-131 activity by the total cellular volume (number of cells multiplied by the average cell volume) gave the cellular activity concentration for each sample. The absolute Cs-131 uptake varied from experiment to experiment. Therefore, for each experiment, the activity concentration was normalized to its value at 380 min for HeLa cells and 480 min for V79 cells. These time points were chosen by convenience, as they were available for most data sets.

Release of Cs-131 from the cells

HeLa and V79 cells grown in 48-well plates were incubated with Cs-131 (~20 kBq/ml) for 13–16 h, at 37 °C, 5% CO_2, to allow cells to accumulate Cs-131. Thereafter, the cells were washed and incubated with fresh growth medium, not containing any Cs-131 for up to 10 h. Cells were washed with PBS, trypsinized (0.1% trypsin/0.5 mM EDTA in PBS for 3-5 min, at 37 °C, 5% CO_2) and resuspended in growth medium. The number of cells, their size and the Cs-131 activity in each sample were measured. Data were normalized to the cellular activity concentration measured when Cs-131 was removed from the cells.

Inhibition of cellular Cs-131 uptake

HeLa and V79 cells grown in 48-well plates were washed with PBS and incubated for 5–6 h in Cs-131 containing medium (~20 kBq/ml) with added ouabain octahydrate (Sigma Aldrich; HeLa: 0 nM 10 nM, 50 nM, 0.1 μM, 0.5 μM, 1 μM, 5 μM; V79: 0 μM, 10 μM, 50 μM, 0.1 mM, 0.5 mM, 1 mM). The cells were washed in PBS, trypsinized (0.1% trypsin containing 0.5 mM EDTA in PBS at 37 °C, 5% CO_2 for 3–5 min) and resuspended in growth medium. The number of cells, their size and the Cs-131 activity in each sample were measured.

Dosimetry

Cell culture geometry

The height of the cellular monolayer (CM), the nuclear shape and the size of HeLa and V79 cells were determined using confocal microscopy. Cells were seeded on high precision cover glasses with a thickness of 0.17 ± 0.01 mm and grown to full confluence overnight at 5% CO_2 and 37 °C. The plasma membrane was stained with 5 μg/ml Germ Agglutinin (WGA) Oregon Green® 488, (Thermo Fisher scientific), in growth medium for 10-20 min at 5% CO_2 and 37 °C. The nuclei were stained with 20 μg/ml Hoechst 33342 (Sigma-Aldrich) in growth medium for 10–20 min at 5% CO_2 and 37 °C. Cells were washed in Hank's Balanced Salt Solution (HBSS; Thermo Fisher Scientific). The staining and imaging were performed on living cells submerged in HBSS. The microscope used was a Laser Scanning Microscope (LSM 780) from Carl Zeiss provided and operated by the Core Facility for Integrated Microscopy, at the University of Copenhagen, Denmark. Seventy-one pictures of the HeLa cell culture were taken, with a spacing of 0.37 μm, covering an axial length of 26.08 μm. Fifty-nine pictures with a spacing of 0.37 μm, covering an axial length of 21.6 μm were taken of the V79 cell culture. The height of the cell layer and the sizes and shapes of the nuclei were determined afterwards using the Zeiss ZEN-lite software package (version 2.3, Carl Zeiss, Germany) operating directly on the *Z*-stack images. The top and bottom positions of the cell layer were evident by a sudden drop in the fluorescent intensity and the appearance of plasma membrane in the form of green spots 'overlying' the nuclei. The height was taken as the distance between these two positions given by the inbuilt scale in the ZEN software. The shape of the nucleus was assumed an ellipsoid. The maximum lengths of the axes in the horizontal plane were measured for each nucleus using the ZEN software. The length of the vertical axis was defined by the 'distance' between the top and bottom position at which the nuclei appeared and disappeared from the images. Of a total of 30 HeLa nuclei and 58 V79 nuclei fully visible in the images, the geometry of 29 HeLa nuclei and 50 V79 nuclei were determined.

Formalism of S_C-values: S_C(N←CM)

The S_C-values was developed for a 100% confluent CM in which the cell nuclei are dispersed (Figure 1). However, they can also be used for an 80% confluent monolayer (as exemplified in the γH2AX experiment), with only small changes in the dosimetry (described later). Cs-131 is equally dispersed throughout the cell (cytoplasm and nucleus) and thereby in the whole cell layer, given a geometry of a vertical cylinder, whose radius is much greater than its height. The assumption of the homogeneous distribution of Cs-131, will be elaborated on in the discussion section. The cell layer had a height of 10 μm for HeLa and 7.5 μm for V79 cells. The horizontal dimension of the cell layer can be considered as infinite: with 1 cm it was much longer than 21 μm, the longest-range electrons emitted by Cs-131 (Table 1). In our calculations, the CM is the radioactive source compartment,

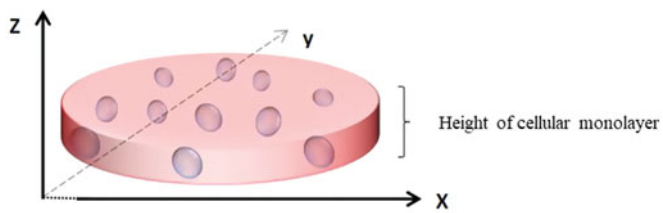

Figure 1. Representation of the cell culture geometry used for S_C-value calculations. The flat cylinder represents the 100% confluent cellular monolayer. The ellipsoids dispersed within it represent the nuclei. The S_C-value, S_C(N←CM), calculates the absorbed dose to the nucleus (target), from the entire cellular monolayer (source).

Table 1. Electron spectrum of Cs-131 decay.

Cs-131 decay, electron spectrum					
Branch	Energy (keV)	Range (μm)	Average LET (keV/μm)	Yield (%)	Energy/decay (keV/Bq s)
Auger_KXY	33.0	21		0.29	
Auger_KLX	28.7	17		2.7	
Auger_KLL	24.4	13		6.0	
'Long' range (>10 μm)	**26.0**	**14**	**1.8**	**9.0**	**2.3**
Auger_LXY	4.72	0.76		1.3	
Auger_LMX	4.00	0.58		18	
Auger_LMM	3.29	0.42		61	
Medium range (0.1–1 μm)	**3.5**	**0.5**	**7.6**	80	**2.8**
Auger_MXY	0.484	0.025		168	
CK_LLX	0.315	0.015		14	
Short range (10–100 nm)	**0.33**	**0.02**	**21**	262	**0.9**
CK_MMX	0.104	0.004		0.68	
CK_NNX	0.0489	0.002		76	
Auger_NXY	0.027	0.001		509	
SCK_NNN	0.012	0.001		94	
Very short range (<10 nm)	**0.037**	**0.002**	**22**	**680**	**0.3**
All	**0.612**			**1018**	**6.2**

CK: Coster-Kronig; SCK: Super Coster-Kronig.

while the cell nucleus (N) takes the role of target region. Such combination is symbolized as S_C(N←CM). The unit of the S_C-value is pl^{-1}·Gy/(Bq s).

A detailed spectrum of the electron energies for Cs-131 decay (Table 1) was provided by Boon Lee, and calculated as previously described in (Lee et al. 2016). Cole's empiric range parameterization in matter with 1 g/cm^3 density (Cole 1969) was used to estimate the range. Monoenergetic electron emission dose kernels for a point source were calculated using the same method applied by MIRD for cellular *S*-values, i.e. by using Cole's empiric stopping power formula (Cole 1969; Goddu et al. 1997). Electrons with energies below 1 keV, were assumed to deposit all their energy at the decay site. A composite dose kernel was made by addition of the individual kernels weighted by their emission probability. Further elaborations on dose kernel computations can be found in (Siragusa et al. 2017).

In order to calculate the S_C-values, we need information on the 3D energy deposition pattern within the modeled cell layer. To get that, the composite dose kernel was convoluted with an activity concentration matrix (Bq/pl), representing the cell layer itself. The S_C-values were always calculated for an activity concentration of 1 Bq/pl, giving each voxel in the cell layer the value 8×10^{-6} pl. Convolution was done in 3D-cartesian coordinates using $(0.2 \times 0.2 \times 0.2)$ μm^3 voxels. The three dimensional 'convn' function in MATLAB (version R2018a, The Mathworks, Inc., Natick, MA, USA) was used. A symmetrical boundary condition with reflection at the lateral boundaries was used, corresponding to an infinite extension of the cell layer. The part of the dose kernels extending in the vertical dimensions, was considered as lost energy and did not contribute to dose. The resulting dose matrix was expressed as (keV/μm^3)/(Bq s)/pl, and converted to Gy/(Bq s)/pl, assuming a density of 1 g/cm^3.

S_C-values for nuclei with different geometries, obtained as described in the *Cell culture geometry* section, were considered. A 'meshgrid' matrix with the same dimensions as the dose matrix was made and the nuclei were placed in the center of it. The meshgrid matrix was turned into a logical matrix, by assigning voxels 'within' the nuclei the value of one and voxels 'outside' the nuclei the value zero. The logical matrix and the dose matrix were then multiplied. The S_C-value is then calculated by dividing the sum of the elements of the resulting matrix, by the number of elements contained in the logical matrix.

The direct X-ray dose contribution to the cell nuclei from Cs-131 (present intracellularly or in the medium) could safely be ignored, as the cell layer thickness is very small compared with the mean free path of the relevant X-ray photons (the mean free path of 29–34 keV photons in water is around 3 cm).

The geometry used for the calculations of S_C-values for γH2AX was an 80% confluent CM. Cells were described as rectangular parallelepipeds with dimensions of 14 μm × 14 μm × 5 μm (length, width, height). Cells were separated by a distance of 1.6 μm, representing the medium, resulting in a surface area covered 80% by cells and 20% by medium. The Cs-131 activity concentration in the medium was set to 1/30 of the activity concentration in the cells as this was the measured difference in Cs-131 concentration between HeLa cells and the medium.

Intracellular absorbed dose calculations

The absorbed dose to the nucleus in the clonogenic cell survival assay depends on both the uptake and release kinetics of Cs-131, while the absorbed dose to the nucleus in the γH2AX assay only depends on the uptake kinetics.

The intracellular activity concentration was measured at the time point where the cells were removed from the Cs-131 containing medium and either processed for the γH2AX assay or seeded for the clonogenic cell survival assay. The Cs-131 activity concentration values, $A(t)$ were fitted to the formula:

$$A(t) = A_0 \cdot (1 - e^{-t \cdot k_a}) \quad (1)$$

using the least square method. A_0 is the cellular activity concentration at equilibrium. The accumulation constant (k_a) was determined by the kinetic studies. k_a is not to be confused with the classical influx rate constant, as k_a depends on both the uptake and release of Cs-131 from the cell. The cumulated cellular Cs-131 activity to any time point is calculated as follow:

$$A^* = \int_0^{t_c} A_0 \cdot (1 - e^{-t \cdot k_a}) dt \quad (2)$$

for cells in γH2AX assay.

$$A^*(t) = \int_0^{t_c} A_0 (1 - e^{-t \cdot k_a}) dt + \int_{t_c}^{1440} A_0' \cdot e^{-t' \cdot k_{out}} dt' \quad (3)$$

$$\text{With } t' = t - t_c$$

for cells in clonogenic cell survivalwhere A_0' is the cellular activity concentration when the Cs-131 containing medium is removed from the cells at time t_c. k_{out} is the rate constant for Cs-131 release from the cells. The absorbed dose for the

clonogenic assay were calculated for 24 h (1440 min). This was seen as a reasonable time span considering the cell cycle time of HeLa and V79 cells and the small amount of Cs-131 left in the cells after 24 h. The absorbed dose to the nucleus is the cumulated activity, A^*, times the S_C-value

$$\text{Absorbed dose} = A^* \cdot S_C(\text{N} \leftarrow \text{CM}) \quad (4)$$

The S_C-values used in the absorbed dose calculations were 8.45×10^{-4} Gy/(Bq s)/pl for HeLa and 8.06×10^{-4} Gy/(Bq s)/pl for V79. The S_C-value used in the absorbed dose calculation for the 80% confluent HeLa cell layer was 7.9×10^{-4} Gy/(Bq s)/pl.

Irradiations

HeLa and V79 cells were seeded in 48-well plates (Sarstedt, Nümbrecht, Germany) and grown overnight to reach 100% confluence (cells used in γH2AX assay were only 80–100% confluent). After exposure, cellular viability, cell number and sizes were obtained using the Count and Viability Kit for the Muse cell analyzer (Merck Millipore, MA, USA), according to the manufacture's protocol and the Scepter 2.0 from Millipore.

Internal radiation exposure with Cs-131

Cells were incubated in 200 μl growth medium containing Cs-131 at activity concentrations of ~15 MBq/ml (HeLa) or ~7.5 MBq/ml (V79) for 420 min or 480 min. After incubation, the cells were washed with PBS, trypsinized (0.1% trypsin/0.5 mM EDTA in PBS for 3–5 min, at 37 °C, 5% CO_2) and resuspended in growth medium. The number of cells, their size and the Cs-131 activity were measured. In addition, cell number and viability were obtained using the Count and Viability Kit and the Muse cell analyzer (Merck Millipore, MA, USA), according to the manufacturer's protocol.

External radiation exposure with γ-rays

The reference exposures were performed using a Cs-137 γ-ray source (5 TBq at time of irradiation, from Canberra Nucomat Universal Calibrator System, Canberra, Australia). Cells were exposed in 200 μl growth medium in a small CO_2 incubator (compact Midi-40, VWR). The dose rate was controlled by varying the distance to the source, in order to match the dose rate profile of the internal Cs-131 exposures. Dose rates between 22 and 490 mGy/h could be achieved this way. After 360 or 480 min of exposure, cells were washed with PBS and trypsinized (0.1% trypsin/0.5 mM EDTA in PBS for 3–5 min, at 37 °C, 5% CO_2). Cells for clonogenic cell survival were seeded in appropriate numbers in T-25 flasks (VWR, Søborg, Denmark) and further exposed to γ-rays for a total of 24 h exposure.

Assays to measure radiotoxicity

γH2AX

The γH2AX assay was performed on HeLa cells using the 'Muse', a small table top flow cytometer (Merck Millipore, Billerica, MA) and the H2A.X Activation Dual Detection Kit (Merck Millipore, Billerica, MA, USA). The cells were treated according to the protocol provided by the manufacturer with minor modifications. Approximately 100,000 cells were transferred to Eppendorf tubes and spun down at 300 g for 5 min. The supernatant was discarded, and the pellet was re-suspended in 100 μl assay buffer. The cells were centrifuged again for 5 min at 300 g, before being re-suspended in a mixture of 100 μl assay buffer and 100 μl fixation buffer. Fixation was performed on ice for 5 min, whereafter the cells were spun down (300 g, 5 min), and the fixation buffer removed. Cells were re-suspended in 200 μl assay buffer and stored at 4 °C for 1–3 days to allow pooling of all samples, (cells exposed to Cs-131 or the reference radiation), before performing the immunostaining and analysis. The cells were spun down (at 300 g, 5 min) and the supernatant removed. They were re-suspended in 200 μl ice cold permeabilization buffer and incubated on ice for 5 min. Thereafter the cells were centrifuged (300 g, 5 min), before the permeabilization buffer was removed and the cells re-suspended in 90 μl assay buffer. 25 μl (50 μl in total) of each of the two antibodies, directed against the non-phosphorylated histone H2AX (anti-Histone H2A.X-PECy5 conjugated antibody) and the phosphorylated serine-139 H2AX (anti-phospho-Histone H2A.X (Ser139)-Alexa Fluor®555) were added to the cells. To the negative control, only the anti-Histone H2A.X-PECy5 conjugated antibody was added. The cells were incubated in the dark for 30 min at room temperature. 100 μl of assay buffer was added to the cells, before they were centrifuged (300 g, 5 min) and the supernatant removed. The cells were washed one more time in 200 μl assay buffer, before being re-suspended in a suitable amount (100–200 μl) of assay buffer and analyzed on the Muse cell analyzer from Merck Millipore (Merck Millipore, Billerica, MA, USA). One thousand cells were analyzed in each sample. The assay was always done 'in pair', so cells exposed to Cs-131 and cells exposed to γ-rays, were stained and analyzed together. Based on the relative fluorescent intensity of the two antibodies, the cells were divided into three categories; activated (γH2AX positive), inactivated (γH2AX negative) and non-expression (H2AX negative). The thresholds were set manually for each 'experimental pair', so the amount of inactivated cells were similar in the two controls. The γH2AX responses were evaluated as the increase in activated cells over control levels.

Clonogenic cell survival

Appropriate numbers of viable cells were seeded in T25 flasks and incubated at 37 °C, 5% CO_2 for 7–9 days (V79) or 14 days (HeLa) to allow for colony formation. The cells were washed with PBS before fixation and staining using 0.25% or 0.5% (w/v) Crystal Violet in methanol (Sigma Aldrich) for at least 30 min. The cells were washed in tap water and

dried, before scoring. Cells that had formed colonies, consisting of at least 50 cells, were defined as survivors (Puck and Marcus 1956).

Results

Production of Cs-131

Using natural barium as target in the form of (25 mg carbonate, i.e. 17.4 mg barium) and 10 days for transport/decay before first Cs-131 extraction, 80 MBq Cs-131 was obtained. However, with an enriched Ba-130 target of 0.15 mg nitrate, 500 MBq Cs-131 was obtained from the first extraction. Cs-131 harvesting has been repeated up to four times on each neutron activated sample. No difference was seen in the purity or the cellular uptake profile whether the Cs-131 came from enriched or natural barium targets. In principle, the specific activity should approach carrier free conditions in both methods.

Cellular kinetics of Cs-131

Uptake of Cs-131 by the cells

The cells took up and accumulated Cs-131 when added to the growth medium. The intracellular concentration of Cs-131 increased until it reached equilibrium (Figure 2).

The cellular activity concentration of Cs-131 were 30 and 70 times higher in HeLa and V79 cells respectively, compared to the Cs-131 activity concentration in the medium. The absolute Cs-131 uptake varied from experiment to experiment, depending on several parameters e.g. the initial Cs-131 activity concentration in the medium. The cellular activity concentrations (at different time points) were therefore normalized to the activity concentration at 380 min (for HeLa cells) and 480 min (for V79 cells). These two time points were chosen to include as many data sets as possible but had otherwise no effect on the obtained results. To find the rate at which Cs-131 accumulated in the cells (k_a), the data were fitted to the function:

$$A(t) = A_0 \cdot (1 - e^{-t \cdot k_a}) \quad (5)$$

using MATLAB Curve Fitting Toolbox (version 3.5.7, The Mathworks, Inc., Natick, MA, USA). $A(t)$, being the normalized activity concentration in the cells at time (t) and A_0, the normalized activity concentration in cells at equilibrium. The obtained values for A_0 and k_a are presented in Table 2.

Release of Cs-131 from the cells

The release of Cs-131 from HeLa and V79 cells is presented in Figure 3. Data were normalized to the cellular activity concentration measured when Cs-131 was removed from the cells and fitted using MATLAB (Curve Fitting Toolbox) to the function:

$$A(t) = A_0 \cdot e^{-t \cdot k_{out}} \quad (6)$$

$A(t)$, being the fraction of Cs-131 left in the cells at time (t) and A_0, the Cs-131 activity concentration in the cells at time point zero. The obtained values for A_0 and k_{out} are presented in Table 2.

Inhibition of cellular Cs-131 uptake

The cellular distribution of Cs-131 is important for the dosimetric calculations. To ensure that Cs-131 was taken up by the cells as ions, and not externally bound to the plasma membrane, we investigated whether the Cs-131 uptake could be inhibited. By blocking the Na^+/K^+-ATPase using ouabain we could inhibit the Cs-131 uptake by 88% in HeLa cell and 72% in V79 cells. The data were fitted to the sigmoid

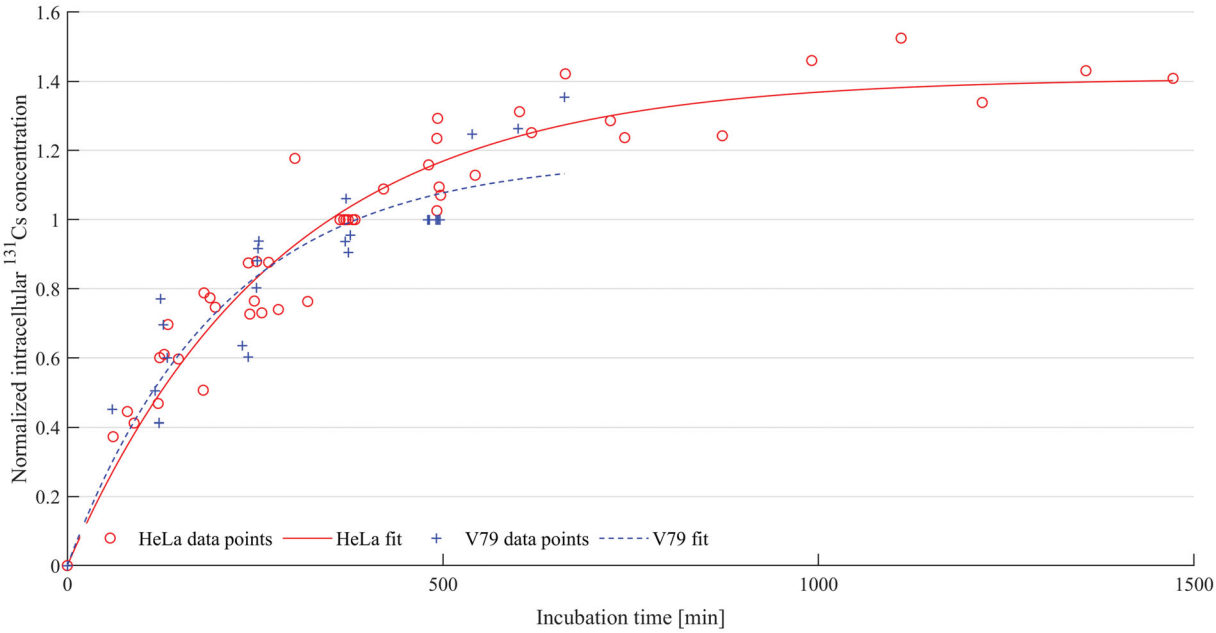

Figure 2. Cellular uptake of Cs-131. Normalized intracellular Cs-131 activity concentration over time in HeLa (○) and V79 (+) cells. Data show the normalized intracellular activity concentration of Cs-131 at time t, relative to the intracellular activity concentration at time point 380 min (HeLa, A380) or time point 480 min (V79, A480). The data were obtained by seven (V79) and eight (HeLa) independent experiments.

Table 2. Cs-131 biokinetic.

Uptake						
Cell line	A_0	95% confidence interval	k_a (min^{-1})	95% confidence interval	SSE	RMSE
HeLa	1.41	1.34–1.48	1/283	1/251–1/325	0.41	0.087
V79	1.18	1.04–1.32	1/204	1/303–1/154	0.35	0.119
Release						
Cell line	A_0	95% confidence interval	k_{out} (min^{-1})	95% confidence interval	SSE	RMSE
HeLa	1.01	0.96–1.06	1/338	1/381–1/304	0.086	0.060
V79	1.03	0.99–1.07	1/256	1/280–1/237	0.064	0.049

SSE: sum of squares due to error; RMSE: root mean squared error.

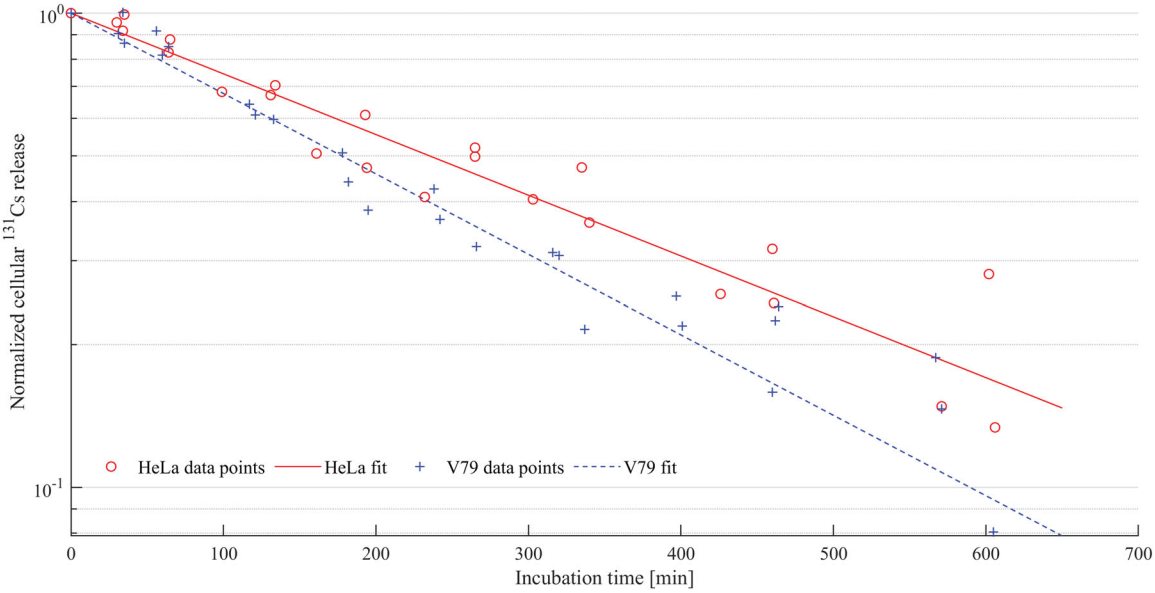

Figure 3. Cellular Cs-131 release. Decrease in intracellular Cs-131 activity concentration over time in HeLa (○) and V79 (+) cells. The data show the fraction of Cs-131 left in the cells per cell volume at time t, compared to time point zero. The data were obtained by three independent experiments.

function:

$$f(x) = \text{Bottom} + \frac{(\text{Top} - \text{Bottom})}{1 + 10^{x - \text{Log}(\text{IC}_{50})}} \quad (7)$$

using in GraphPad prism 7.03 and are presented in Figure 4. The results confirm that Cs-131 is transported into the cells as ions and accumulated intracellularly.

Dosimetry

Cell culture geometry

The height of the CMs and the sizes of the nuclei were determined by confocal microscopy. A cross section of the 100% confluent CM can be seen in Figure 5. As is evident from the illustration, neighboring cells are so close to each other that their plasma membranes (green) are touching, leaving no space between them. A high cell density is central for the geometry assumed in the S_C-value calculations and its verification is important for correct absorbed dose calculations. The average heights of the confluent cell layers were determined to be 10 μm for the HeLa cell culture and 7.5 μm for the V79 cell culture, with an estimated uncertainty of ± 1–2 μm due the variations in cellular height (as evident from Figure 5) and to limitations of the confocal microscopy technique. The cell cultures used for the clonogenic assay had this level, 100%, of confluence, while the cell cultures used for the γH2AX assay were 80% confluent.

Vertical dose distribution

When the cell culture is 100% confluent and Cs-131 is equally distributed throughout the whole cell (cytoplasm and nucleus), the dose distribution in the cell layer in the horizontal plane is constant (except for small edge effects near the wall of the cell culture well). The dose distribution on the vertical axis varies as shown in Figure 6. The dose distribution in the middle of the cell layer will approach the constant infinite volume approximation, corresponding to a S_C-value of 9.94×10^{-4} Gy/(Bq s)/pl. The height of the cell layer was difficult to determine precisely. Therefore the effect on the dose distribution due to changes in this height was examined. The axial dose distribution for CMs with heights of 6 μm, 7.5 μm, 10 μm and 12 μm, either including or ignoring the dose contribution from the medium, are shown in Figure 6. Due to the high accumulation of Cs-131 in the cells, the dose contribution from Cs-131 present in the medium is small and can safely be ignored.

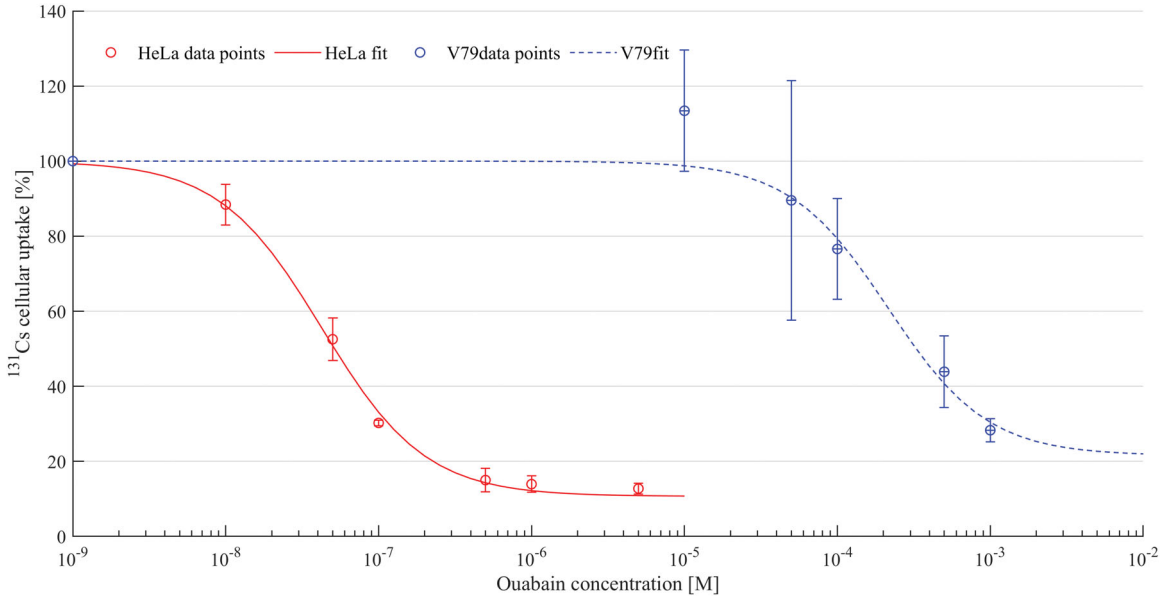

Figure 4. Inhibition of Cs-131uptake. Inhibition of Cs-131 uptake by ouabain in HeLa cells (○) and V79 cells (+). Circles represent the average ± standard deviation (s.d.) of three independent experiments. IC50 (the ouabain concentration needed to inhibit the uptake by 50%) and the maximum achievable inhibition were estimated (by GraphPad prism) to be 2.6×10^{-8} M and ~11% respectively for HeLa cells and 2.77×10^{-4} M and ~7% for V79 cells. ($R^2 = 0.917$ (HeLa), $R^2 = 0.890$ (V79)).

S_C-values

S_C-values (N←CM) for 29 (HeLa) and 50 (V79) nuclei, whose volume was estimated based on the images obtained by confocal microscopy, were calculated (Figure 7). In general, the nuclei displayed an ellipsoid shape rotated at different angles in respect to the horizontal plane. The volume of the cell nuclei ranged from 0.1 to 1.6 pl with a mean of 0.84 ± 0.30 pl (s.d.) for HeLa cells and from 0.1 to 1.4 pl with a mean of 0.53 ± 0.24 pl (s.d.) for V79 cells.

The non-constant axial dose distribution (Figure 6) will result in variation of the S_C-values for nuclei of different volumes and rotations. These variations are however small as the axial dose distribution is relatively 'flat'. The variation between the S_C-values of the different nuclei is below 1% for HeLa cells and below 7.5% for V79 cells, even though the volumes of the nuclei differ by a factor of 10. As shown in Figure 7, the S_C-values are almost independent of the nuclear volume.

The cell layer height was estimated to be 10 ± 2 μm and 7.5 ± 2 μm respectively for the HeLa and V79 cell cultures. To investigate the influence of the uncertainty of the height of the cell layer, S_C-values for the HeLa and V79 nuclei were calculated using a height of 12 μm, 10 μm, 7.5 μm and 6 μm. On average the S_C-values decreased by 8% for HeLa nuclei when the height of the cell layer was changed from 12 μm to 7.5 μm and by 10% for V79 nuclei when the height was changed from 10 μm to 6 μm (data not shown).

Radiotoxicity of Cs-131

To demonstrate the usefulness of the 'new' radionuclide Cs-131, the experimental setup and the S_C-values, we investigated the radiotoxicity of intracellular Cs-131 decays using γH2AX and the clonogenic cell survival.

γH2AX assay

HeLa cells were exposed either to intracellular Cs-131 decays or to external γ-rays (reference radiation). To avoid a dose rate effect, the dose rate profile for the two exposures were matched, as described in the methods section. The γH2AX response increased with the absorbed dose, reaching a 3.5 fold increase (compared to control levels) after receiving ~5-6 Gy over 8 h of exposure. The γH2AX response was similar for the two exposures and no difference in the radiotoxicity was observed (Figure 8).

Clonogenic cell survival

Cells were exposed to either intracellular Cs-131 or to γ-rays (reference radiation) at similar dose rates. The HeLa cells were allowed to form colonies for 14 days before scoring. The V79 cells exposed to intracellular Cs-131 were incubated for 7 days, while the V79 cells exposed to the reference radiation were incubated 1–2 days longer (8–9 days). This extended amount of time for colony formation after γ-ray exposure cells can cause an overestimation of the RBE value for the V79 cells (Figure 9).

The HeLa cells were only exposed over a small range of absorbed doses. It was therefore not possible to see the presence of a potential shoulder on the survival curves. The data were therefore fitted to the linear model ($y = e^{-\alpha x}$). This was also the case for the V79 cells exposed to reference radiation. However, the data points for the Cs-131 exposed V79 cells show a clear linear survival curve. The exact shape of survival curves depends on several experimental parameters and comparison with earlier published results are therefore difficult. However, considering the lower dose rate used in this study the observed radiation sensitivity of the V79 cells to γ-rays is comparable to what we found in earlier experiments published in (Siragusa et al. 2017).

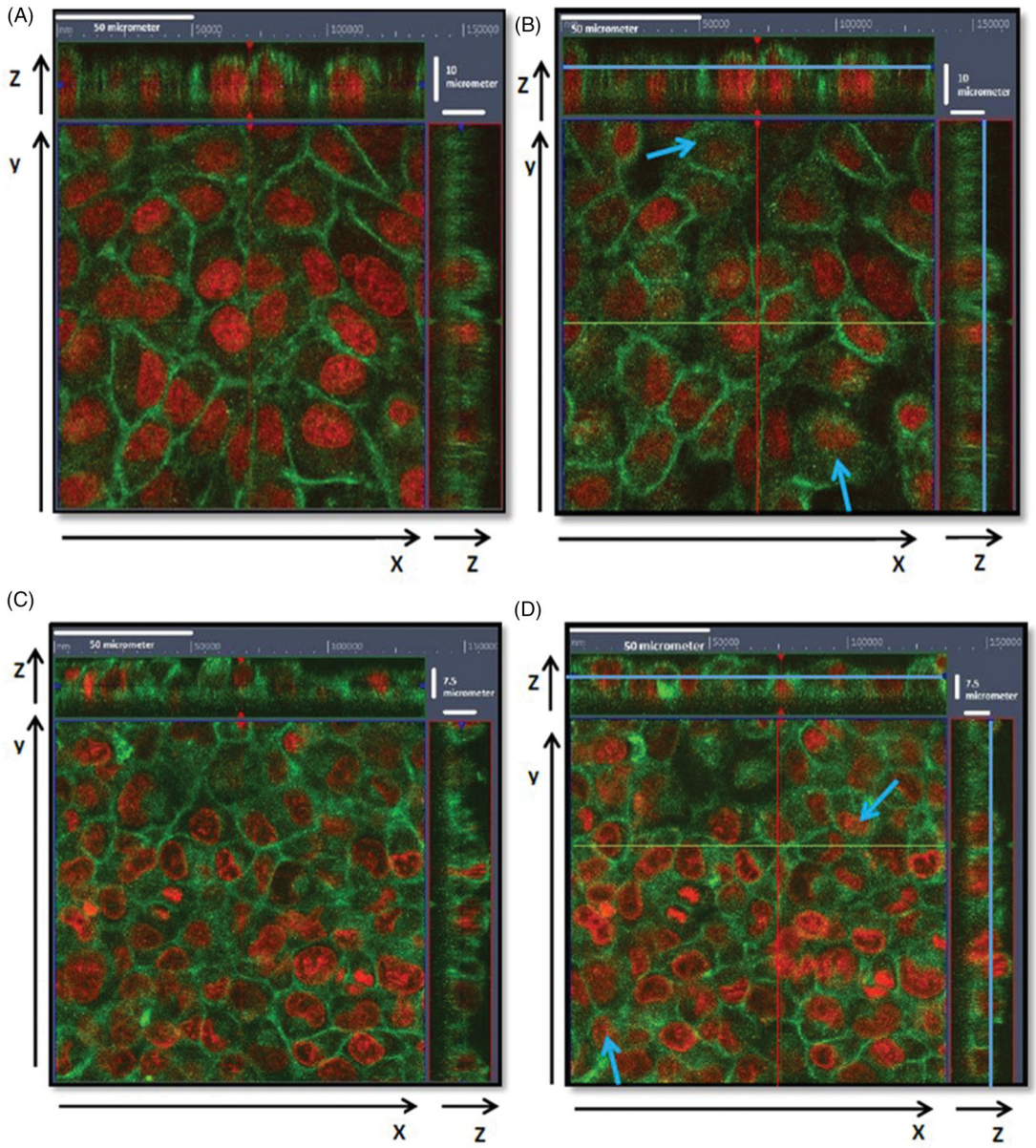

Figure 5. Illustration of confocal microscopy images of the cellular monolayer in culture. Confocal images of HeLa (A,B) and V79 (C,D) cell cultures. The plasma membrane (green) and nuclei (red) were stained with WGA Oregon green 488 (5 μg/ml) and Hoechst (20 μg/ml) respectively for 10–20 min at 5% CO_2, 37 °C. The color was digitally changed from blue to red. Pictures were acquired by confocal laser scanning microscope (LSM 780) from Zeiss, using a 10× objective. All geometrical measurements were taken directly in Zeiss ZEN software on the original pictures, which were richer in contrast and details. Panels A and C show a cross section (*x*–*y* plane) in the middle of the cellular monolayer. Panels B and D shows the estimated 'top' of the cellular monolayer in the *x*–*y* plane. The red and green lines indicate the position of the cross section in the *z* plane visible in the 'picture bars' (*x*–*z* plane (red) and *y*–*z* plane (green)). The blue arrows show the presence of plasma membrane (green spots) 'on top' of the nuclei (red). The blues lines in the 'picture bars' indicate the position of the estimated top in the *z*-plane. The average monolayer height was estimated to be 10 μm for the HeLa cell culture and 7.5 μm V79 cell culture.

Both the survival curves for the Cs-131 exposed cells and the γ-ray exposed cells were described by the linear model and the RBE is simply the ratio of the slopes of the two curves. An RBE value of 3.9 was found for intracellular Cs-131 decays in HeLa cells and a RBE of 3.2 was found for V79 cells.

Discussion

In this study, we examined the potential of a 'new' radioisotope, Cs-131, for investigating the radiotoxicity of Auger-electrons emitters in vitro. We studied the bio-kinetics of Cs-131 in HeLa and V79 cells. Based on the results, we developed and demonstrated an experimental setup as well as a new type of cellular *S*-values: the S_C-values. By combining these tools, the dosimetry becomes both remarkably simple and robust. We demonstrated the usefulness of this setup for investigating the RBE for intracellular Cs-131 Auger decays.

First, we have confirmed that Cs-131 can be made readily available without use of expensive enriched isotopes. The repeated generator-like precipitate extraction lends itself well to campaigns of radiation biology experiments. The required radiochemistry procedures and tools are simple and should

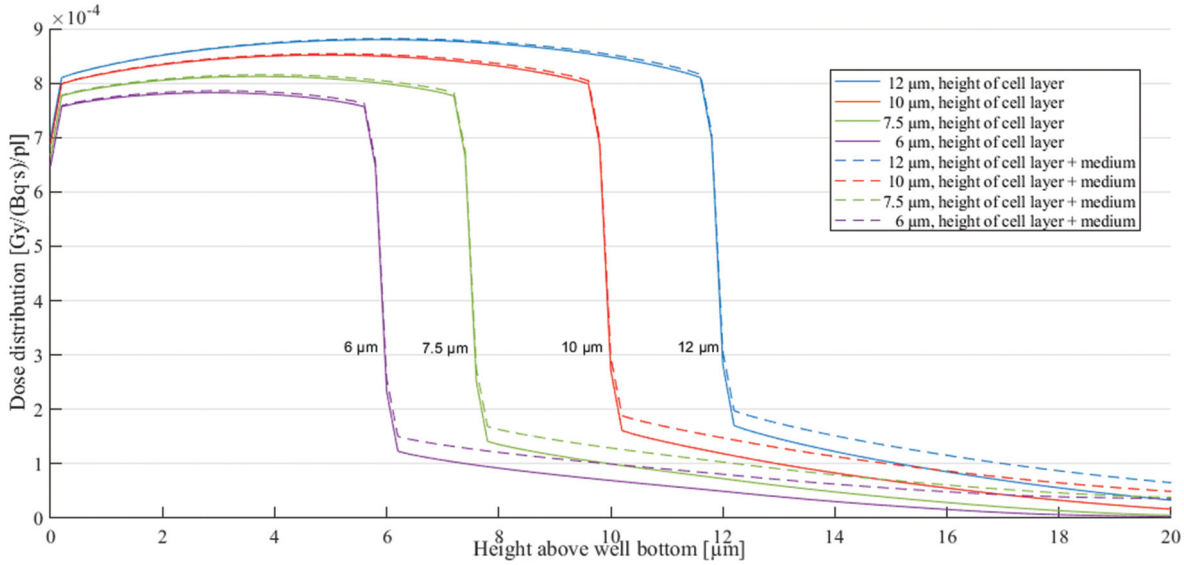

Figure 6. Axial dose distributions for cellular monolayers of different heights. The axial dose distribution for cellular monolayers of different heights (6 μm, 7.5 μm, 10 μm and 12 μm) either ignoring or including the dose contribution from the medium is shown. A cellular accumulation factor of 30 for Cs-131 was used in the calculations. The 'bottom' of the cell layers is located at 0 μm, while the estimated top of the cell layer (used in S_C-value calculations) for HeLa and V79 cells is located at 10 μm and 7.5 μm, respectively. The maximum point dose for each of the cell layer heights were 8.80×10^{-4}, 8.51×10^{-4}, 8.12×10^{-4} and $7.82 \cdot 10^{-4}$ Gy/(Bq s)/pl, respectively.

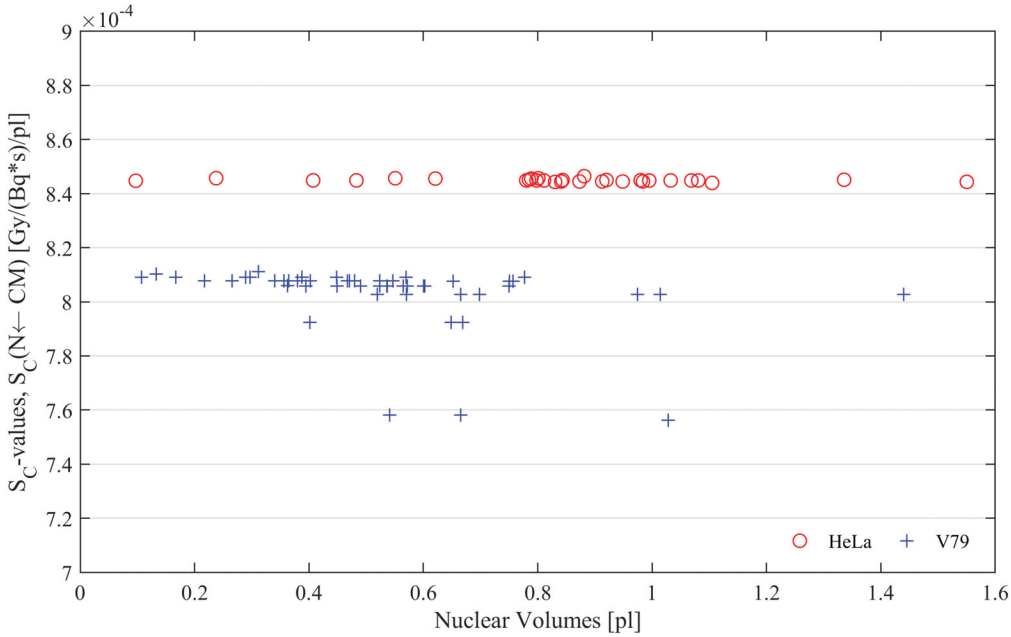

Figure 7. S_C-values for HeLa and V79 nuclei. The S_C-values (S_C(N←CM)) for the HeLa nuclei (○) ranged from $8.44 \cdot 10^{-4}$ Gy/(Bq s)/pl to $8.46 \cdot 10^{-4}$ Gy/(Bq s)/pl. The S_C-values for the V79 nuclei (+) ranged from $7.56 \cdot 10^{-4}$ Gy/(Bq s)/pl to $8.11 \cdot 10^{-4}$ Gy/(Bq s)/pl. Differences in the S_C-values for nuclei of similar volumes are due to differences in the lengths of their individual axes and to different orientations of the nuclei. Cellular monolayers with a height of 10 μm (HeLa) and 7.5 μm (V79), ignoring the dose contribution from the medium, were used in the calculations.

be almost universally available. We found a *first-principles* way to calculate relevant S_C-values for realistic cell geometries in culture, taking advantage of the homogeneous distribution of the isotope in the cell. The simple cellular kinetic of Cs-131 and the robust dosimetry made this setup useful in studying and quantifying the Auger effect in vitro without the dosimetric uncertainties that come with more complicated Auger experiments setups.

Cellular kinetics of Cs-131

Cs-131 was taken up by cells in a predictable manner when it was added to the medium. The cellular uptake and release of Cs-131 followed a first order kinetics, in which the Cs-131 uptake and release depends linearly on the initial Cs-131 concentration. Although the exact mechanism of the cellular uptake for Cs-131 is not of prime importance for the use as a cellular level radiobiology tool, we have tried to

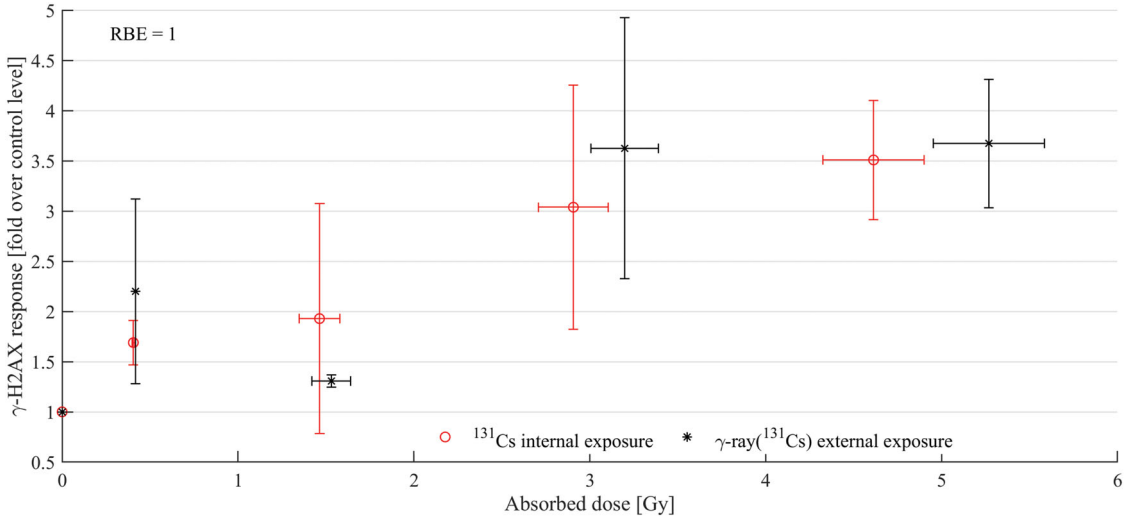

Figure 8. γH2AX response in HeLa cells after exposure to intracellular Cs-131 or external γ-rays (reference radiation). HeLa Cells were exposed to either intracellular Cs-131 decays (○) or external γ-rays (*) at similar dose rate profiles. γH2AX response is plotted as fold over the control levels as a function of absorbed dose. Data are presented as average ± s.d. of 2–3 independent experiments.

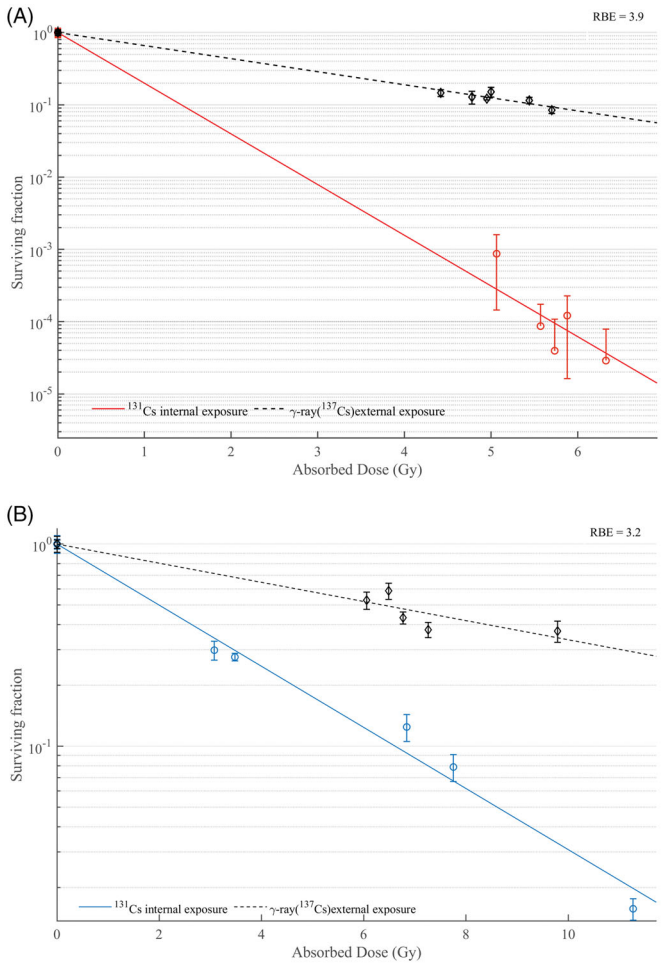

Figure 9. Clonogenic cell survival after exposure to intracellular Cs-131 or external γ-rays (reference radiation). Clonogenic cell survival as a function of absorbed dose for HeLa (A) and V79 (B). Cells exposed to intracellular Cs-131 (solid lines) or external γ-rays from Cs-137 (dashed lines; reference radiation) at similar dose rate profiles are shown. The survival curves were fitted to the linear model (HeLa: ($y = e - 1.62x$ Cs-131 exposed cells; $y = e - 0.416x$ reference radiation); V79: $y = e - 0.348x$ Cs-131 exposed cells; $y = e - 0.109x$ reference radiation)). The data points were obtained by three independent experiments and presented as average ± s.d. of three replicates.

support the basic assumption of cesium being pumped across the cell membrane by Na^+/K^+-ATPase as earlier proposed (Whittam and Ager 1964; Davis et al. 1988). Ouabain is a well-known inhibitor of this pump. We were able to partly block the Cs-131 uptake when ouabain was added to the Cs-131 containing medium in a concentration of 10^{-6} M (HeLa) or 10^{-3} M (V79), resulting in a threefold (V79) to eightfold (HeLa) lower cesium uptake. Increasing the ouabain concentration above 10^{-6} M did not have any further reducing effect on the cesium uptake in HeLa cells. Due to the vital importance of the Na^+/K^+-ATPase and the cellular toxicity of ouabain (Suhail 2010), a complete blocking of this pump is not feasible, and we did not attempt to block the uptake any further. It is likely that the 'remaining' Cs-131 is still transported by this pump or other potassium channels present in the mammalian plasma membrane (Aabert et al. 2002). It is also possible that Cs^+ ions are able to penetrate the plasma membrane without transport through any channels (Shirai et al. 2013). Importantly, the uptake of Cs-131 by the Na^+/K^+-ATPase confirms that Cs-131 is transported into the cells in its ionic form. As Cs^+ ions, due to their chemistry, do not bind to cellular constituents, they must remain as ions. This is of significance for the argumentation of the homogeneous intracellular distribution of Cs-131. Aqueous water-filled channels (part of the nuclear pore complex), located in the nuclear envelope, allow small metabolites, proteins and ions to diffuse freely in both directions between the cytoplasm and the nucleus (Knockenhauer and Schwartz 2016). With an effective diameter in the order of nanometers (Samudram et al. 2016) these pores easily allow (even hydrated) Cs^+ to move freely between the two compartments, resulting in a homogeneous distribution of Cs-131 activity throughout the cell. An identical distribution of cesium and potassium has been experimentally confirmed by synchrotron-radiation induced X-ray fluorescence (SR-XRF) of plant cells (Ortega 2005; Isaure et al. 2006). A homogeneous distribution of potassium, after proper normalization for mass density variations, has also

been confirmed for numerous mammalian cells. Thus it has been demonstrated that potassium is indeed equidistributed in fibroblasts, (Zierold et al. 1984), human ovarian cancer (IGROV-1; Devès and Ortega 2002) and yeast (Ortega et al. 2004), pheochromocytoma (PC12; Kosior et al. 2012), and human phagocytic cells (Gramaccioni et al. 2018). Together these studies support the assumption of a homogeneous intracellular distribution of Cs-131. We note that a study in amphibian oocytes found a significant enhancement of K^+ concentration in the cells' nuclei (Dick 1978). However, these huge cells have hundred times larger linear dimensions and about one million times larger volumes than the mammalian cells studied in the present work and the K^+ concentration gradient observed by (Dick 1978) seems not representative for our work. It is noteworthy that the techniques of SR-XRF, or electron- or proton-microprobe induced X-ray emission respectively, usually require fixation of the cells prior to the measurement. Dedicated comparisons found that chemical fixation methods and air-drying of the cells may modify the content of mobile elements such as alkali ions, while this issue does not occur with cryo-fixation (Perrin et al. 2015; Jin et al. 2017). A novel method using genetically encoded fluorescent probes even enables potassium imaging in life cells and one group reported a significant K^+ concentration enhancement in the nucleus of HeLa cells (Bischof et al. 2017), while another group using slightly different fluorescent probes did not highlight such a variation (Shen et al. 2019). Future studies of the intracellular distribution of alkali ions and in particular of cesium would be beneficial to corroborate our basic assumption of their homogeneous intracellular distribution or, respectively, provide reproducible distribution data to adapt the dosimetry calculations accordingly.

Dosimetry

The geometry used to calculate the S_C-values was a 100% confluent CM (except for the γH2AX assay where it was 80%). As Cs-131 was homogeneously distributed throughout the cells, the activity concentration in the whole cell culture is the same. The dose distribution in the cell culture must therefore depend only on the height of the cell layer. However, as seen in Figure 6, changes in this height only had a small effect on the dose distribution. Similarly, the S_C-values for HeLa and V79 nuclei are remarkably 'stable' within a range of biological and experimental variations in nuclei sizes and shapes (Figure 7). This stability exists even when the uncertainty of the cell layer height is considered. The stability in S_C-values is due to the geometry of the cell layer used, and to the unit of the S_C-values, being expressed as Gy/(Bq s)/pl. By expressing the S_C-values as Gy/(Bq s)/pl, (instead of Gy/(Bq s) as known from the MIRD cellular S-values), the total number of decays in the cells is normalized to their volumes. The normalized cumulative activity is then used in the absorbed dose calculations. In an infinite activity pool, the S_C-values would be totally independent of the size of the nuclei and have a value of 9.94×10^{-4} Gy/(Bq s)/pl (for all nuclei).

Experimental setup

With the robust S_C-values and the simple and known uptake and release kinetics of Cs-131, it is easy to plan and obtain the desired absorbed doses and dose rates for an experiment. From direct cell measurements, we have found the activity per cell sample (as function of time), the total number of cells and the cell volume (as a statistical distribution). With this, supplemented with our knowledge of the kinetics, the activity per cell volume and, the cumulated activity at any time in the experiment can be calculated. An achieved cumulated activity of 8.000 Bq s, corresponding to an absorbed dose of 6 Gy could be reached within 8 h.

Using this setup, clonogenic cell survival curves and γH2AX dose effect curves were produced for V79 and HeLa cells. Dose-rate controlled RBE values were calculated for intracellular Cs-131 exposure. The maximum concentration of cesium used was 35 nM (4.6 ng Cs gram of solution), which is less than the typical cesium levels in human tissue (Williams and Leggett 1987) and a cytotoxic effect of cesium can therefore be ruled out. No increase in effectiveness of Cs-131 compared to external γ-rays was observed in HeLa cells for the phosphorylation of histone H2AX (RBE = 1). Nevertheless, from the clonogenic cell survival data, RBE values of 3.2 and 3.9 were found for intracellular Cs-131 decays in V79 and Hela cells, respectively. These RBE results should be seen as preliminary and prove that the experimental setup can be used to study radiation induced biological effects. We have to interpret them with the caveat that the γ-ray exposed V79 cells had 1 or 2 days more time to form colonies than the Cs-131 treated cells and therefore an overestimation of the RBE value cannot be ruled out. The lower RBE value obtained by γH2AX compared to clonogenic cells survival, can be a result of the relatively low expression of H2AX histones (2% of the total H2A histones) in HeLa cells (Bonner et al. 2008). Or it can simply be a result inherent in different methods applied. Indeed, RBE values for high LET radiation, obtained by detection of DNA dsb are often lower than RBE values obtained by other methods (Prise et al. 1998). This has also been observed for Auger emitters (Kriehuber et al. 2004).

The activity concentration of Cs-131 in the cells and so the absorbed dose and dose rate depends only on the activity concentration of Cs-131 in the medium and so the desired absorbed doses and dose rates can be obtained by adjusting the Cs-131 activity added to the medium. This points to a future extension of this method for the measurement of DNA damage from semi-chronic exposure to low levels of intracellular Auger emitters especially relevant in radiation protection. The easily controllable dose rate allow for an experimental setup in which the dose rate can be matched to other (externally) available sources. This is of great advantage for experiments in which the quantitative effect of Auger-electron emitters is compared to other types of radiation for example when investigating RBE-values as it is done here. Further, the method can be used with many different exposure modifications to study the effect of hypoxia, scavengers, dose-rate, drugs, cell types and so forth.

As evident by the different k_a and k_{out} for HeLa and V79 cells, the kinetic time constants differ between the two cell types and so these constants will have to be determined individually as shown. However, the Na^+/K^+-ATPase, by which Cs-131 is transported, is present in the plasma membrane of all mammalian cells (Suhail 2010), and so the experimental setup can easily be used for other mammalian cell lines than HeLa and V79 cells. The transport of K^+ across the cell membrane or cell wall is vital for an organism's ability to maintain its membrane potential (Suhail 2010), and Cs-131 can be expected to be transported into other cell types or organisms, by a variety of K^+ transporters. These cells/organisms include non-mammalian cells (Latorre and Miller 1983), bacteria (Zhang et al. 2014), algae (Avery et al. 1991, 1993) and fungi (Avery 1995).

The S_C-values presented here with the same beneficial features, can also be calculated for other radionuclides than Cs-131 and the experimental setup can be modified to include these. The main requirement is the homogeneous inter- and intra-cellular distribution of the radionuclide. The dose contribution from the medium depends on the accumulation factor and the electron energies. However, as long as the activity concentration in the cells is at least the same as in the medium, it will in general either be neglectable or contribute to the 'stabilization' of the S_C-values.

Conclusion

In this study, we investigate the bio-kinetics of Cs-131 uptake by a cell culture model and use it to investigate the radiotoxicity of Auger emitters. To the best of our present knowledge, cesium is quite evenly distributed throughout the cell. It thus constitutes a 'dumb' Auger-therapy agent but is excellently suited for studies of the biological response. The robust dosimetry circumvents the high uncertainty in the absorbed dose calculations, related to biological variations in cell and nuclei sizes and shapes, which might mask the 'real' biological response to Auger electrons. Our method is relatively simple to establish and lends itself to many different exposure modifications (dose-rate, oxygen level, scavengers, cell types) and possibly also other radionuclides. We therefore believe it will be an important new tool for the necessary investigation of the underlying mechanism behind the biological effect of Auger-electron emitters.

Acknowledgements

The authors thank Boon Quan Lee from Department of Nuclear Physics at Australian National University, Canberra, for theoretical calculation of the Cs-131 Auger-electron energies and yields. The authors acknowledge the Core Facility for Integrated Microscopy (CFIM), Department of Biomedical Science, University of Copenhagen for help with confocal microscopy of the cell cultures.

Disclosure statement

The authors report no conflicts of interest.

Notes on contributors

Pil M. Fredericia is a postdoctoral researcher at the Technical University of Denmark (DTU). She is investigating the biological response of low-energy electrons with a special focus on relative biological effectiveness (RBE) of Auger-electron emitters

Mattia Siragusa is a postdoctoral researcher at the Technical University of Denmark (DTU). He is involved in cellular dosimetry calculations for low-energy electrons and in the development of computer-vision-based automated cell colony counters.

Gregory Severin is a nuclear physicist and radiochemist with special focus on isotope production and radionuclide purification. Of particular interest are the use of rare earth radiometals for diagnostics and therapeutics use in invasive diseases.

Ulli Köster is an experimental physicist at the Institut Laue-Langevin, Grenoble. He works in experimental nuclear physics and production of non-conventional medical isotopes.

Torsten Groesser is a researcher at the Technical University of Denmark (DTU). He is a biophysicist with experience in performing ionizing radiation experiments using low- and high-LET radiation including radioisotopes to study *in-vitro* radiation responses.

Mikael Jensen is a professor in applied nuclear physics at the Technical University of Denmark (DTU). He is an experimental nuclear physicist, with special focus on medical isotope production and radiochemistry.

ORCID

Pil M. Fredericia http://orcid.org/0000-0002-2824-0626
Mattia Siragusa http://orcid.org/0000-0002-4028-1404
Gregory Severin http://orcid.org/0000-0003-1189-7311
Torsten Groesser http://orcid.org/0000-0003-3143-1906
Mikael Jensen http://orcid.org/0000-0002-9109-2187

References

Aabert B, Johnson A, Lewis J, Raff M, Roberts K, Walter P. 2002. Molecular biology of the cell. 4th ed. New York: Garland Science.

Avery S, Codd G, Gadd G. 1993. Transport kinetics, cation inhibition and intracellular location of accumulated caesium in the green microalga *Chlorella salina*. J Gen Microbiol. 139:827–834.

Avery SV, Codd GA, Gadd GM. 1991. Caesium accumulation and interactions with other monovalent cations in the cyanobacterium Synechocystis PCC 6803. J Gen Microbiol. 137:405–413.

Avery SV. 1995. Caesium accumulation by microorganisms: uptake mechanisms, cation competition, compartmentalization and toxicity. J Ind Microbiol. 14:76–84.

Bischof H, Rehberg M, Stryeck S, Artinger K, Eroglu E, Waldeck-Weiermair M, Gottschalk B, Rost R, Deak AT, Niedrist T, et al. 2017. Novel genetically encoded fluorescent probes enable real-Time detection of potassium in vitro and in vivo. Nat Commun. 8:11.

Bonner WM, Redon CE, Dickey JS, Nakamura AJ, Sedelnikova OA, Solier S, Pommier Y. 2008. GammaH2AX and cancer. Nat Rev Cancer. 8:957–967.

Cole A. 1969. Absorption of 20-eV to 50,000-eV electron beams in air and plastic. Radiat Res. 38:7–33.

Costantini DL, Chan C, Cai Z, Vallis KA, Reilly RM. 2007. ^{111}In-labeled trastuzumab (Herceptin) modified with nuclear localization sequences (NLS): an Auger electron-emitting radiotherapeutic agent for HER2/neu-amplified breast cancer. J Nucl Med. 48:1357–1368.

Davis D, Murphy E, London R. 1988. Uptake of cesium ions by human erythrocytes and perfused rat heart: a cesium-133 NMR study. Biochemistry. 27:3547–3551.

Devès G, Ortega R. 2002. Subcellular mass determination by $^4He^+$ energy-loss micro-spectrometry. Anal Bioanal Chem. 374:390–394.

Dick DA. 1978. The distribution of sodium, potassium and chloride in the nucleus and cytoplasm of *Bufo bufo* oocytes measured by electron microprobe analysis. J Physiol (Lond). 284:37–53.

Feinendegen L, Ertl H, Bond V. 1971. Biological toxicity associated with the Auger effect. In: Biophysical aspects of radiation quality. Vienna (Austria): IAEA; p. 1689–1699.

Goddu SM, Howel RW, Bouchet LG, Bloch WE, Rao D. 1997. MIRD cellular S values. Reston (VA): Society of Nuclear Medicine.

Gramaccioni C, Yang Y, Procopio A, Pacureanu A, Bohic S, Malucelli E, Iotti S, Farruggia G, Bukreeva I, Notargiacomo A, et al. 2018. Nanoscale quantification of intracellular element concentration by X-ray fluorescence microscopy combined with X-ray phase contrast nanotomography. Appl Phys Lett. 112:053701.

Hoang B, Reilly RM, Allen C. 2012. Block copolymer micelles target Auger electron radiotherapy to the nucleus of HER2-positive breast cancer cells. Biomacromolecules. 13:455–465.

Hofer K, Hughes W. 1971. Radiotoxicity of intracellular tritium, ^{125} iodine and ^{131} iodine. Radiat Res. 47:94–109.

Isaure MP, Fraysse A, Devès G, Le Lay P, Fayard B, Susini J, Bourguignon J, Ortega R. 2006. Micro-chemical imaging of cesium distribution in Arabidopsis thaliana plant and its interaction with potassium and essential trace elements. Biochimie. 88:1583–1590.

Jin Q, Paunesku T, Lai B, Gleber SC, Chen S, Finney L, Vine D, Vogt S, Woloschak G, Jacobsen C. 2017. Preserving elemental content in adherent mammalian cells for analysis by synchrotron-based x-ray fluorescence microscopy. J Microsc. 265:81–93.

Kassis A. 2004. The amazing world of Auger electrons. Int J Radiat Biol. 80:789–803.

Kassis AI, Adelstein SJ. 2005. Radiobiologic principles in radionuclide therapy. J Nucl Med. 46:4S–12S.

Kassis AI. 2003. Cancer therapy with Auger electrons: are we almost there? J Nucl Med. 44:1479–1481.

Knockenhauer KE, Schwartz TU. 2016. The nuclear pore complex as a flexible and dynamic gate. Cell. 164:1162–1171.

Kosior E, Bohic S, Suhonen H, Ortega R, Devès G, Carmona A, Marchi F, Guillet JF, Cloetens P. 2012. Combined use of hard X-ray phase contrast imaging and X-ray fluorescence microscopy for subcellular metal quantification. J Struct Biol. 177:239–247.

Kriehuber R, Riedling M, Simkó M, Weiss DG. 2004. Cytotoxicity, genotoxicity and intracellular distribution of the Auger electron emitter ^{65}Zn in two human cell lines. Radiat Environ Biophys. 43:15–22.

Latorre R, Miller C. 1983. Conduction and selectivity in potassium channels. J Membr Biol. 71:11–30.

Lee BQ, Nikjoo H, Ekman J, Jönsson P, Stuchbery AE, Kibédi T. 2016. A stochastic cascade model for Auger-electron emitting radionuclides. Int J Radiat Biol. 92:1–13.

Leyton JV, Hu M, Gao C, Turner P, Dick JE, Minden M, Reilly RM. 2011. Auger electron radioimmunotherapeutic agent specific for the CD123+/CD131- phenotype of the leukemia stem cell population. J Nucl Med. 52:1465–1473.

NuDat2.7. 2004. Release 2.7. National Nuclear Data Center (NNDC). New York: Brookhaven National Laboratory. [accessed 2019 March]. http://www.nndc.bnl.gov/nudat2/chartNuc.jsp

Ortega R, Bohic S, Tucoulou R, Somogyi A, Devès G. 2004. Microchemical element imaging of yeast and human cells using synchrotron X-ray microprobe with Kirkpatrick-Baez optics. Anal Chem. 76:309–314.

Ortega R. 2005. Chemical elements distribution in cells. Nucl Instrum Meth Phys Res B. 231:218–223.

Perrin L, Carmona A, Roudeau S, Ortega R. 2015. Evaluation of sample preparation methods for single cell quantitative elemental imaging using proton or synchrotron radiation focused beams. J Anal at Spectrom. 30:2525–2532.

Prise KM, Ahnström G, Belli M, Carlsson J, Frankenberg D, Kiefer J, Löbrich M, Michael BD, Nygren J, Simone G, et al. 1998. A review of DSB induction data for varying quality radiations. Int J Radiat Biol. 74:173–184.

Puck TT, Marcus PL. 1956. Action of X-rays on mammalian cells. J Exp Med. 103:653–666.

Samudram A, Mangalassery BM, Kowshik M, Patincharath N, Varier GK. 2016. Passive permeability and effective pore size of HeLa cell nuclear membranes. Cell Biol Int. 40:991–998.

Shen Y, Wu SY, Rancic V, Aggarwal A, Qian Y, Miyashita SI, Ballanyi K, Campbell RE, Dong M. 2019. Genetically encoded fluorescent indicators for imaging intracellular potassium ion concentration. Commun Biol. 2:18.

Shirai O, Ohnuki T, Kitazumi Y, Kano K. 2013. Transport of cesium ion across a bilayer lipid membrane and its facilitation in the presence of iodide ion. Electroanalysis. 25:1823–1826.

Siragusa M, Baiocco G, Fredericia PM, Friedland W, Groesser T, Ottolenghi A, Jensen M. 2017. The COOLER Code: a novel analytical approach to calculate subcellular energy deposition by internal electron emitters. Radiat Res. 188:204–220.

Suhail M. 2010. Na, K-ATPase: ubiquitous multifunctional transmembrane protein and its relevance to various pathophysiological conditions. J Clin Med Res. 2:1–17.

Ussing H. 1959. The alkali metal ions in isolated systems and tissues. In: Eichler O, Farah A, editors. Handbuch der experimentellen pharmakologie (Ergänzungswerk). 13th ed. Berlin: Springer; p. 1–29.

Whittam R, Ager M. 1964. Vectorial aspects of adenosine-triphosphatase activity in erythrocyte membranes. Biochem J. 93:337–348.

Williams LR, Leggett RW. 1987. The distribution of intracellular alkali metals in Reference Man. Phys Med Biol. 32:173–190.

Williams R. 1970. Tilden Lecture. The biochemistry of sodium, potassium, magnesium, and calcium. Q Rev Chem Soc. 24:331–365.

Zhang P, Idota Y, Yano K, Negishi M, Kawabata H, Arakawa H, Morimoto K, Tsuji A, Ogihara T. 2014. Characterization of cesium uptake mediated by a potassium transport system of bacteria in a soil conditioner. Biol Pharm Bull. 37:604–607.

Zierold K, Schafer D, Pietruschka F. 1984. The element distribution in ultrathin cryosections of cultivated fibroblast cells. Histochemistry. 80:333–337.